Bol. Soc. Paran. Mat.
©SPM – E-ISSN-2175-1188
SPM: www.spm.uem.br/bspm

(3s.) **v. 2026 (44) 4** : 1–20.
ISSN-0037-8712
doi:10.5269/bspm.79960

Exploring Topological Indices and QSPR Models for Anti-Cancer Drugs

Naveen S. Sapare*, Sudhir R. Jog, V. G. Hiremath, Vishwanath A. Modagi

ABSTRACT: This research examines the utilization of topological indices (TIs) and Quantitative Structure–Property Relationship (QSPR) models to delineate the physicochemical features of five anti-cancer pharmaceuticals: Adriamycin, Carboplatin, Carmustine, Ellence, and Hydroxyurea. Employing chemical graph representations, M-polynomials (M-P) and neighborhood M-polynomials (NM-P) were formulated to calculate a set of degree-based (DB) and neighborhood degree sum-based (NDSB) topological indices (TIs). After that, linear, quadratic, and cubic regression models were used to find relationships between these indices and ten important physicochemical parameters. The analysis shows that several TIs, such the Second Zagreb index, Forgotten topological index, Harmonic index, and Symmetric division index, can be used to forecast parameters like molar weight, half-life, polar surface area, density, and refractive index. The findings indicate that quadratic and cubic models typically surpass linear models in prediction accuracy, as evidenced by low RMSE values that validate strong structure–property correlations. The results show that polynomial-derived DB and NDSB TIs are an effective way to study structure-property connections, which can help with rational drug design and the creation of new anti-cancer treatments.

Key Words: M-polynomial, NM-polynomial, degree-based topological indices, regression model, QSPR analysis, anti-cancer drugs.

Contents

1. Introduction

Cancer is the term used to describe the body's aberrant cells' increased penetration. Carcinogens are substances that cause cancer. A chemical substance that comprises specific components and is present in cigarette smoke is called a carcinogen. It can spread to other parts of the body. A lump, weight loss, irregular bleeding, and coughing are just a few of this condition's numerous symptoms.

The primary causes of this malignant illness include chronic tobacco chewing, obesity, poor diet, indolence, and excessive alcohol usage. This serious illness can be treated with a variety of drugs, such as hormone treatment, chemotherapy, surgery, and others. This disease is treated with anticancer medications, which include metabolites and alkylates.

For the past two to three decades, the world has been dealing with the possibility of discovering a cure for cancer. Millions of people worldwide suffer with this illness each year. The drugs used to treat cancer a malignant disease, are known as anticancer treatments. There are many kinds of anticancer drugs, including hormones, antimetabolites, and alkalizing agents. Numerous studies have demonstrated a strong correlation between anticancer drugs and the chemical structures of alkanes. In this proposed effort, several TIs created for anticancer drugs to help researchers comprehend their physical characteristics and associated chemical interactions. Additionally, covered is the QSPR analysis of nine degree-based topological markers. We further show that the features are closely related to the physiochemical properties of anticancer medicines Chemical Graph Theory is concerned with graphs that

* Corresponding author.

Submitted November 07, 2025. Published February 03, 2026
2020 *Mathematics Subject Classification:* 05C92, 05C09, 92E10

depict chemical systems. Topological Indices (TI s) for anticancer drugs can be computed using chemical graph theory. A mathematical formula that can be used to characterize any network that depicts a molecule structure is the topological graph index, also referred to as a molecular descriptor. H. Wiener originally calculated and presented the study on the graph G's TIs in 1947 [1].

This work employs some pharmaceuticals, and a number of well-defined distinct TIs are on a variety of anticancer medications that estimate their physical properties and associated chemical processes using degree-based computations [2]. Topological indices are useful tools for studying the physiochemical properties of chemical compound structures.

Numerous indices have since been examined in the literature [3,4,5]. Graph theory is the subject where we extract the information present in the graph using many polynomials such as, Hosoya polynomial, Pi polynomial [6,7,8] M-Polynomial and NM polynomial [9,10,11,12]. The M-P and NM-P are the most efficient polynomials to extract information from the graph. The topological index may be used to analyze mathematical values and explore various physical characteristics of a molecule.

In 2015, E. Deutsch and S. Klavžar [13] gave the explanation for general M-P for the graphs.

$$M(G) = \sum_{a \leq b} m_{ab}(G)\, x^a y^b, \quad \text{where } m_{ab} \text{ is the overall number of edges } uv$$

refers to the pair of vertices belongs to the edge set $E(G)$. M. C. Shanmukha [14] shown usage of M-P and NM-P methodology to study four antiviral medications Remedesivir, Chloroquine, Hydroxychloroquine and Theaflavin involved in the diagnosis of COVID-19 and breast cancer patients. Syed Ajaz K. Kirmani [15], worked to assess the efficiency of various DB and NDSB TIs of drugs Lopinavir, Ritonavir, Arbidol, and Thalidomide through M-P and NM-P which are used to treat COVID-19, also used some physiochemical attributes and biological activity of the medications investigated to test the predictive strength of these Degree Based and Neighbourhood Degree Based TIs. Using combinatorial computation and edge partition technique. Syed Ahtsham Ul Haq Bokhary [16], Özge Çolakoğlu Havare [17] worked on numerous promising drugs. The expressions of M-P and NM-P for numerous prospective medications, including Triciferol, Vorinostat, Tucidinostat, HDCA-based CUDC-101, and CUCD-907 multi-target therapies, are established for these pharmaceuticals by examining their molecular structures and QSPR models for various physiochemical properties feature of the medications mentioned above, which are viewed as crucial in cancer treatment. They also used degree and neighborhood degree counting methods to obtain the results.

All of this inspires us to study the molecular structure of Adriamycin(A), Ellence(E), and Carboplatin(Cb), Hydroxyurea(H), Carmustine(Cm) all of which are utilized to treat cancer. For chemical graphs of these medications, M-P and NM-P based on DB and NDSB respectively and QSPR analysis depending on the total number of degrees surrounding vertices are constructed or developed. Also, in [18] TIs are discussed using the multiple regression analysis. Different models are generated based on NDSB TIs and physiochemical properties of various cancer treating medicines.

This research linear, quadratic, and cubic regression models to analyze the relationship between topological indices and the physicochemical properties of selected anticancer drugs. The simplest way to figure out how structure influences molecular properties is to utilize linear regression. Chemical behavior is frequently nonlinear due to several molecular characteristics, including branching, heteroatoms, steric effects, and connectivity patterns. To further understand these kinds of nonlinear interactions, we incorporated quadratic and cubic polynomial regressions. We can also see the trade-off between complexity and how well the forecast works by slowly boosting the polynomial degree. The correlation got better and the RMSE values went down when we switched from linear to higher-order models. This shows that polynomial regression is better for figuring out how the structure and properties of these compounds are related. These regression approaches also make sure that the findings are straightforward to understand and don't have the difficulties with overfitting that are common in more complicated machine learning models. So, the regression methods that were chosen are the optimum mix of being simple to use, quick to compute, and accurate for early-stage QSPR study.

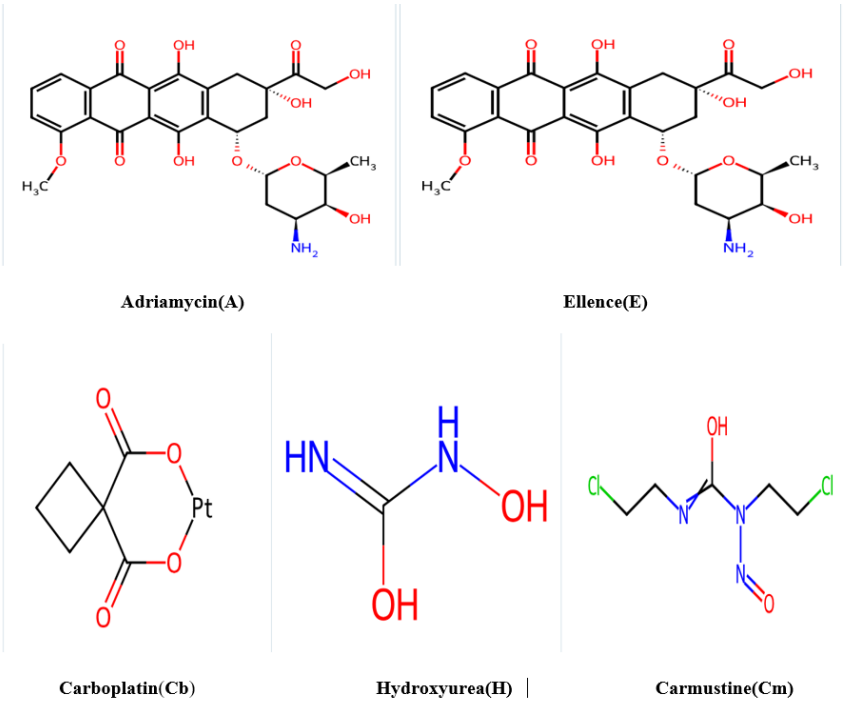

Figure 1: Molecular Structure of five anticancer drugs

2. Preliminaries

In the beginning, we go over the graph-theoretic ideas and polynomial tools that we employed in this study. We use a finite simple graph $G = (V, E)$ to show each drug molecule. The vertices of the graph are atoms, and the edges are covalent bonds. The degree of a vertex equals the number of edges that touch it. We also look at the neighborhood degree-sum of a vertex, which is the sum of the degrees of its nearby vertices. This gives us second-order connectivity information about an atom. The M-polynomial $M(G) = \sum_{a \leq b} m_{ab}(G)\, x^a y^b$ shows the joint degree distribution at the ends of edges, where $m_{ab}(G)$ is the number of edges connecting vertices with degrees a and b. The NM-polynomial does the same thing for the distribution of neighborhood degree-sums at edge endpoints. By using simple differential and substitution operators on these polynomials and then evaluating them at $x = y = 1$, we may get many often used topological indices, such as the Zagreb indices, the forgotten index, the harmonic index, and the symmetric division index. We find degree-based (DB) and neighborhood-degree-sum based (NDSB) indices from $M(G)$ and $NM(G)$ and use them as descriptors in QSPR models (linear, quadratic, and cubic regressions) to look into the structure–property relationships of the five anticancer drugs we looked at: Adriamycin, Carboplatin, Carmustine, Ellence, and Hydroxyurea.

Adriamycin (Doxorubicin): Adriamycin is an anthracycline antibiotic used in chemotherapy. Its chemical formula is $C_{27}H_{29}NO_{11}$. It works by intercalating DNA strands, inhibiting DNA and RNA synthesis, and generating free radicals. It is frequently used to treat several cancers, such as lymphoma, bladder cancer, and breast cancer. Side effects can include hair loss, nausea, vomiting, and cardiotoxicity.

Carboplatin: Carboplatin is a platinum-based chemotherapy drug. Its Chemical Formula: $C_6H_{14}N_2O_4$. It works by cross-linking DNA, which inhibits DNA synthesis and cell division. It's used to treat various cancers, including ovarian cancer, lung cancer, and head and neck cancer.

Carmustine: Carmustine also known as BCNU (Bis-chloroethylnitrosourea), has a chemical formula:

$C_5H_9Cl_2N_3O$ It is a chemotherapy medication used primarily in the treatment of certain types of brain tumors, multiple myeloma, Hodgkin's lymphoma, and non-Hodgkin's lymphoma. It works by interfering with the growth of cancer cells and can cross the blood-brain barrier, which makes it particularly effective for brain tumors. Carmustine can also affect normal body cells, leading to. It's administered under strict medical supervision due to its potency and potential side effects.

Ellence(Epirubicin): Ellence is also an anthracycline used in chemotherapy. Its Chemical Formula: $C_{27}H_{29}NO_{11}$. It is similar to doxorubicin but has a different spatial orientation of the hydroxyl group, which may reduce its toxicity. It's used to treat breast cancer, ovarian cancer, and other types of cancer.

Hydroxyurea: Chemical Formula of Hydroxyurea is $C_{14}H_{15}N_3O_3$. It is an antineoplastic drug used to treat certain cancers, such as chronic myeloid leukemia and sickle cell disease. It works by inhibiting ribonucleotide reductase, which decreases DNA synthesis. Side effects can include bone marrow suppression, gastrointestinal symptoms, and skin reaction.

Drugs	**MW**	**MP**	**Pka**	**HL**	**LogP**	**HF**	**BP**	**D**	**PSA**	**RI**
Adriamycin	579.98	212.5	9.5	34	1.3	12.5	523.3	1.22	206.3	1.685
Carboplatin	371.25	200	7.4	17.5	-0.15	9.1	384.4	1.3	114.7	1.7
Carmustine	214.05	61	4.5	1.5	1.4	-43.2	245.3	1.2	52.3	1.6
Ellence	543.5	212.5	9.5	1.75	1.75	12.5	523.3	1.22	206.3	1.685
Hydroxyurea	72.5	136	8.3	3	-1.32	-71.9	265.3	1.48	69.72	1.56

Table 1: Physicochemical Properties of Anti Cancer Drugs [19]

3. Computational Work

In this part we derive the expressions of M-P and NM-P of the molecular graphs of Adriamycin(A), Carboplatin(Cb), Carmustine(Cm) Ellence(E) and Hydroxyurea(H). Using various combinatorial computation such as edge partition method and neighborhood degree counting method. Molecular graphs are to understand DB and NDSB TIs using [19] for the above anticancer drugs.We also study QSPR of various physiochemical proprties.

Theorem 3.1 Let A be the graph of molecule Adriamycin(A),then

$$\begin{aligned} M(A) &= 2xy^2 + 8xy^3 + 2xy^4 + 2x^2y^2 + 10x^2y^3 + 4x^2y^4 + 14x^3y^3 + 2x^3y^4 \\ NM(A) &= 2x^2y^4 + 2x^3y^6 + 6x^3y^7 + 2x^4y^5 + 2x^4y^7 + 2x^4y^8 + x^5y^7 + x^5y^8 + 4x^6y^6 + 3x^6y^7 + 6x^7y^8 + 6x^7y^9 \\ &\quad + x^7y^{10} + 2x^8y^8 + x^8y^9 + 2x^8y^{10} + x^9y^9. \end{aligned}$$

Proof: The graph of the molecule Adriamycin (A) is represented in Figure 1. The number of vertices is

$$V(A) = 40, \qquad e(A) = 44.$$

From the molecular structure of Adriamycin (A), the edge set is separated into 8 classes based on the degrees of the end vertices.

$$e_{ij} = \{\, uv \in E(A) \mid d(u) = i \text{ and } d(v) = j \,\}, \qquad m_{ij} = |e_{ij}|.$$

That is, m_{ij} denotes the number of edges whose end vertices have degrees i and j. From the molecular graph we obtain:

$$e_{12} = 2, \quad e_{13} = 8, \quad e_{14} = 2, \quad e_{22} = 2, \quad e_{23} = 10, \quad e_{24} = 4, \quad e_{33} = 14, \quad e_{34} = 2.$$

Therefore, the polynomial

$$M(A) = \sum_{i \le j} m_{ij}(A)\, x^i y^j$$

Topological Index	**Formula** $\alpha(\epsilon(u),\epsilon(v))$	**Derivation at** $x=y=1$
1st ZI: $M_1(G)$ and 3rd version ZI: $NM_1(G)$	$\sum_{uv\in E(G)} \big(\epsilon(u)+\epsilon(v)\big)$	$(D_x + D_y)\, f(x,y)$
2nd ZI: $M_2(G)$ and 2nd NZI: $NM_2(G)$	$\sum_{uv\in E(G)} \epsilon(u)\,\epsilon(v)$	$(D_x\, D_y)\, f(x,y)$
2nd MZI: $mM_2(G)$ and 2nd NMZI: $NmM_2(G)$	$\sum_{uv\in E(G)} \dfrac{1}{\epsilon(u)\,\epsilon(v)}$	$(S_x\, S_y)\, f(x,y)$
3rd RZI: $ReZG_3(G)$ and 3rd $ND_3(G)$	$\sum_{uv\in E(G)} \big(\epsilon(u)\,\epsilon(v)\big)\big(\epsilon(u)+\epsilon(v)\big)$	$(D_x\, D_y)(D_x + D_y)\, f(x,y)$
FTI: $F(G)$ and NFTI: $NF(G)$	$\sum_{uv\in E(G)} \big(\epsilon(u)^2+\epsilon(v)^2\big)$	$(D_x^2 + D_y^2)\, f(x,y)$
SDD: $SDD(G)$ and 5th NDe index: $ND_5(G)$	$\sum_{uv\in E(G)} \dfrac{\epsilon(u)^2+\epsilon(v)^2}{\epsilon(u)\,\epsilon(v)}$	$(D_x\, S_y + S_x\, D_y)\, f(x,y)$
HI: $H(G)$ and NHI: $NH(G)$	$\sum_{uv\in E(G)} \dfrac{2}{\epsilon(u)+\epsilon(v)}$	$(2\, S_x\, J)\, f(x,y)$
ISI: $I(G)$ and NISI: $NI(G)$	$\sum_{uv\in E(G)} \dfrac{\epsilon(u)\,\epsilon(v)}{\epsilon(u)+\epsilon(v)}$	$(S_x\, J\, D_x\, D_y)\, f(x,y)$

Table 2: Degree-based topological indices, edge–sum formulas

becomes

$$\begin{aligned} M(A) &= e_{12}x^1y^2 + e_{13}x^1y^3 + e_{14}x^1y^4 + e_{22}x^2y^2 + e_{23}x^2y^3 + e_{24}x^2y^4 + e_{33}x^3y^3 + e_{34}x^3y^4 \\ &= 2xy^2 + 8xy^3 + 2xy^4 + 2x^2y^2 + 10x^2y^3 + 4x^2y^4 + 14x^3y^3 + 2x^3y^4. \end{aligned}$$

Similarly, the edge set based on the *neighborhood degree sum* is categorized into the following 17 classes:

$$e^*_{ij} = \{\, uv \in E(A) \mid nd(u) = i,\ nd(v) = j \,\}, \qquad m^*_{ij} = |e^*_{ij}|.$$

From the structure we obtain:

$$\begin{aligned} &e^*_{24}=2, \quad e^*_{36}=2, \quad e^*_{37}=6, \quad e^*_{45}=2, \quad e^*_{47}=2, \quad e^*_{48}=2, \\ &e^*_{57}=1, \quad e^*_{58}=1, \quad e^*_{66}=4, \quad e^*_{67}=3, \quad e^*_{78}=6, \quad e^*_{79}=6, \\ &e^*_{7,10}=1, \quad e^*_{88}=2, \quad e^*_{89}=1, \quad e^*_{8,10}=2, \quad e^*_{99}=1. \end{aligned}$$

Hence, the polynomial

$$NM(A) = \sum_{i\le j} m^*_{ij}(A)\, x^i y^j$$

becomes

$$\begin{aligned}NM(A) &= e^*_{24}x^2y^4 + e^*_{36}x^3y^6 + e^*_{37}x^3y^7 + e^*_{45}x^4y^5 + e^*_{47}x^4y^7 + e^*_{48}x^4y^8 + e^*_{57}x^5y^7 + e^*_{58}x^5y^8 + e^*_{66}x^6y^6 \\ &\quad + e^*_{67}x^6y^7 + e^*_{78}x^7y^8 + e^*_{79}x^7y^9 + e^*_{7,10}x^7y^{10} + e^*_{88}x^8y^8 + e^*_{89}x^8y^9 + e^*_{8,10}x^8y^{10} + e^*_{99}x^9y^9 \\ &= 2x^2y^4 + 2x^3y^6 + 6x^3y^7 + 2x^4y^5 + 2x^4y^7 + 2x^4y^8 + x^5y^7 + x^5y^8 + 4x^6y^6 + 3x^6y^7 + 6x^7y^8 + 6x^7y^9 + \\ &\quad + x^7y^{10} + 2x^8y^8 + x^8y^9 + 2x^8y^{10} + x^9y^9.\end{aligned}$$

Theorem 3.2 Let A denote the graph representing molecule Adriamycin(A).The various TIs are

S.NO	M-P Index	Value	NM-P Index	Value
1	$M_1(A)$	228	$NM_1(A)$	572
2	$M_2(A)$	286	$NM_2(A)$	1908
3	$mM_2(A)$	8.55	$NmNM_2(A)$	1.4160
4	$ReZG_3(A)$	1596	$ND_3(A)$	27618
5	$F(A)$	652	$NF(A)$	4054
6	$SDD(A)$	108	$ND_5(A)$	97.45
7	$H(A)$	17.705	$NH(A)$	7.2698
8	$I(A)$	52.695	$NI(A)$	137.5879

Table 3: TIs of Adriamycin(A)

Proof: Theorem 3.1 gives

$$(D_x + D_y)M(A) = 6xy^2 + 32xy^3 + 10xy^4 + 8x^2y^2 + 50x^2y^3 + 24x^2y^4 + 84x^3y^3 + 14x^3y^4,$$

$$(D_xD_y)M(A) = 4xy^2 + 24xy^3 + 8xy^4 + 8x^2y^2 + 60x^2y^3 + 32x^2y^4 + 126x^3y^3 + 24x^3y^4,$$

$$(S_xS_y)M(A) = \tfrac{2xy^2}{2} + \tfrac{8xy^3}{3} + \tfrac{2xy^4}{4} + \tfrac{2x^2y^2}{4} + \tfrac{10x^2y^3}{6} + \tfrac{4x^2y^4}{8} + \tfrac{14x^3y^3}{9} + \tfrac{2x^3y^4}{12},$$

$$(D_xD_y)(D_x + D_y)M(A) = 12xy^2 + 96xy^3 + 40xy^4 + 32x^2y^2 + 300x^2y^3 + 192x^2y^4 + 756x^3y^3 + 168x^3y^4,$$

$$(D_x^2 + D_y^2)M(A) = 10xy^2 + 80xy^3 + 34xy^4 + 16x^2y^2 + 130x^2y^3 + 80x^2y^4 + 252x^3y^3 + 50x^3y^4,$$

$$(D_xS_y + S_xD_y)M(A) = 5xy^2 + \tfrac{80}{3}xy^3 + \tfrac{17}{2}xy^4 + 4x^2y^2 + \tfrac{65}{3}x^2y^3 + 10x^2y^4 + 28x^3y^3 + \tfrac{25}{6}x^3y^4.$$

$$2S_xJ(x,y) = 2\left(\tfrac{2x^3}{3} + \tfrac{10x^4}{4} + \tfrac{12x^5}{5} + \tfrac{18x^6}{6} + \tfrac{2x^7}{7}\right),$$

$$S_xJD_xD_y(x,y)(A) = \tfrac{4x^3}{3} + \tfrac{24x^4}{4} + \tfrac{8x^5}{5} + \tfrac{8x^4}{4} + \tfrac{60x^5}{5} + \tfrac{32x^6}{6} + \tfrac{126x^6}{6} + \tfrac{24x^7}{7}.$$

$$\begin{aligned}NM(A) &= 2x^2y^4 + 2x^3y^6 + 6x^3y^7 + 2x^4y^5 + 2x^4y^7 + 2x^4y^8 + x^5y^7 + x^5y^8 + 4x^6y^6 + 3x^6y^7 \\ &\quad + 6x^7y^8 + 6x^7y^9 + x^7y^{10} + 2x^8y^8 + x^8y^9 + 2x^8y^{10} + x^9y^9.\end{aligned}$$

$$\begin{aligned}(D_x + D_y)NM(A) &= 12x^2y^4 + 18x^3y^6 + 60x^3y^7 + 18x^4y^5 + 22x^4y^7 + 24x^4y^8 + 12x^5y^7 + 13x^5y^8 + 48x^6y^6 + 39x^6y^7 \\ &\quad + 90x^7y^8 + 96x^7y^9 + 17x^7y^{10} + 32x^8y^8 + 17x^8y^9 + 36x^8y^{10} + 18x^9y^9,\end{aligned}$$

$$\begin{aligned}(D_xD_y)NM(A) &= 16x^2y^4 + 36x^3y^6 + 126x^3y^7 + 40x^4y^5 + 56x^4y^7 + 64x^4y^8 + 35x^5y^7 + 40x^5y^8 + 144x^6y^6 \\ &\quad + 126x^6y^7 + 336x^7y^8 + 378x^7y^9 + 70x^7y^{10} + 128x^8y^8 + 72x^8y^9 + 160x^8y^{10} + 81x^9y^9,\end{aligned}$$

$$\begin{aligned}(S_xS_y)NM(A) &= \tfrac{2x^2y^4}{2} + \tfrac{2x^3y^6}{18} + \tfrac{6x^3y^7}{4} + \tfrac{2x^4y^5}{20} + \tfrac{2x^4y^7}{28} + \tfrac{2x^4y^8}{32} + \tfrac{x^5y^7}{35} + \tfrac{x^5y^8}{40} + \tfrac{4x^6y^6}{36} + \tfrac{3x^6y^7}{42} + \tfrac{6x^7y^8}{56} + \tfrac{6x^7y^9}{63} \\ &\quad + \tfrac{x^7y^{10}}{70} + \tfrac{2x^8y^8}{64} + \tfrac{x^8y^9}{72} + \tfrac{2x^8y^{10}}{80} + \tfrac{x^9y^9}{81}.\end{aligned}$$

So that we obtain various TIs as in Table 3 from the above equations by taking $x = 1$.

Theorem 3.3 Let us C denote the graph representing the molecule *Carboplatin* (Cb).then,

$$M(C) = 2xy^3 + 2xy^4 + 2x^2y^2 + 2x^2y^3 + 4x^2y^4 + 2x^3y^4.$$
$$NM(C) = 2x^3y^7 + 4x^4y^6 + 2x^6y^7 + 2x^6y^{10} + 2x^7y^7 + 2x^7y^{10}.$$

Proof: The molecular graph of carboplatin is represented in Figure 1. We have,

$$V(C) = 13, \quad e(C) = 14.$$

From the molecular structure of Carboplatin, on the basis of vertex degrees, the edge set is separated into six classes as follows:

$$e_{13} = 2,\ e_{14} = 2,\ e_{22} = 2,\ e_{23} = 2,\ e_{24} = 4,\ e_{34} = 2.$$

Thus,

$$\begin{aligned} M(C) &= \sum_{a\leq b} m_{ab}(C)\, x^a y^b \\ &= e_{13}x^1y^3 + e_{14}x^1y^4 + e_{22}x^2y^2 + e_{23}x^2y^3 + e_{24}x^2y^4 + e_{34}x^3y^4 \\ &= 2xy^3 + 2xy^4 + 2x^2y^2 + 2x^2y^3 + 4x^2y^4 + 2x^3y^4. \end{aligned}$$

Similarly, considering the sum of the degrees of neighborhood vertices, the edge set of Carboplatin is separated into the following seven classes:

$$e^*_{37} = 2,\ e^*_{46} = 4,\ e^*_{47} = 2,\ e^*_{67} = 2,\ e^*_{6,10} = 2,\ e^*_{77} = 2,\ e^*_{7,10} = 2.$$

Hence,

$$\begin{aligned} NM(C) &= \sum_{a\leq b} m^*_{ab}(C)\, x^a y^b \\ &= e^*_{37}x^3y^7 + e^*_{46}x^4y^6 + e^*_{67}x^6y^7 + e^*_{6,10}x^6y^{10} + e^*_{77}x^7y^7 + e^*_{7,10}x^7y^{10} \\ &= 2x^3y^7 + 4x^4y^6 + 2x^6y^7 + 2x^6y^{10} + 2x^7y^7 + 2x^7y^{10}. \end{aligned}$$

Theorem 3.4 Let C be the molecular graph of Carboplatin (Cb). Then, various TIs are:

S.NO	M-P Index	Value	NM-P Index	Value
1	M1(C)	74	NM1(C)	180
2	M2(C)	90	NM2(C)	580
3	mM2(C)	2.67	NmNM2(C)	0.412
4	ReZG3(C)	516	ND3(C)	8144
5	F(C)	226	NF(C)	1260
6	SDD(C)	37.67	ND5(C)	31.03
7	H(C)	5.5047	NH(C)	2.2787
8	I(C)	16.2615	NI(C)	42.9968

Table 4: TIs of Carboplatin (Cb)

Proof: Using Theorem 3.3 and the operators D_x, D_y, S_x, S_y (acting on $M(C)$ or $NM(C)$ as indicated) we obtain the following expressions.

$$(D_x + D_y)M(C) = 8xy^3 + 10xy^4 + 8x^2y^2 + 10x^2y^3 + 24x^2y^4 + 14x^3y^4,$$

$$(D_xD_y)M(C) = 6xy^3 + 8xy^4 + 8x^2y^2 + 12x^2y^3 + 32x^2y^4 + 24x^3y^4,$$

$$(S_xS_y)M(C) = \frac{2xy^3}{3} + \frac{xy^4}{2} + \frac{x^2y^2}{2} + \frac{x^2y^3}{3} + \frac{x^2y^4}{2} + \frac{x^3y^4}{6},$$

$$(D_xD_y)(D_x + D_y)M(C) = 24xy^3 + 40xy^4 + 32x^2y^2 + 60x^2y^3 + 192x^2y^4 + 168x^3y^4,$$

$$(D_x^2 + D_y^2)M(C) = 20xy^3 + 34xy^4 + 16x^2y^2 + 26x^2y^3 + 80x^2y^4 + 50x^3y^4.$$

$$(D_xS_y + D_yS_x)M(C) = \frac{20}{3}xy^3 + \frac{34}{4}xy^4 + 4x^2y^2 + \frac{13}{3}x^2y^3 + 10x^2y^4 + \frac{25}{6}x^3y^4.$$

Next, some auxiliary (integral / summation) identities used in the computations are

$$\begin{aligned} 2\big(S_xJ(x,y)M(C)\big) &= \frac{2(x)^4}{2} + \frac{4x^5}{5} + \frac{2(x)^4}{2} + \frac{4x^5}{5} + \frac{4x^6}{3} + \frac{4x^7}{7} \\ &= 2(x)^4 + \frac{8x^5}{5} + \frac{4x^6}{3} + \frac{4x^7}{7}, \end{aligned}$$

$$S_xJ(D_xD_y)(x,y)M(C) = \frac{14(x)^4}{4} + \frac{20(x)^5}{5} + \frac{32(x)^6}{6} + \frac{24x^7}{7}.$$

We obtain NM polynomial $NM(C)$ expressions:

$$(D_x + D_y)NM(C;x,y) = 20x^3y^7 + 40x^4y^6 + 26x^6y^7 + 32x^6y^{10} + 28x^7y^7 + 34x^7y^{10},$$

$$(D_xD_y)NM(C) = 42x^3y^7 + 96x^4y^6 + 84x^6y^7 + 120x^6y^{10} + 98x^7y^7 + 140x^7y^{10},$$

$$(S_xS_y)NM(C) = \frac{2x^3y^7}{21} + \frac{4x^4y^6}{24} + \frac{2x^6y^7}{42} + \frac{2x^6y^{10}}{60} + \frac{2x^7y^7}{49} + \frac{2x^7y^{10}}{70},$$

$$(D_xD_y)(D_x + D_y)NM(C) = 420x^3y^7 + 960x^4y^6 + 1092x^6y^7 + 1920x^6y^{10} + 1372x^7y^7 + 2380x^7y^{10},$$

$$(D_x^2 + D_y^2)NM(C;x,y) = 116x^3y^7 + 208x^4y^6 + 170x^6y^7 + 272x^6y^{10} + 196x^7y^7 + 298x^7y^{10},$$

$$(D_xS_y + D_yS_x)NM(C) = \frac{116}{21}x^3y^7 + \frac{52}{6}x^4y^6 + \frac{85}{21}x^6y^7 + \frac{136}{30}x^6y^{10} + 4x^7y^7 + \frac{149}{35}x^7y^{10}.$$

Finally, using the operator $S_xJ(D_xD_y)$ on $NM(C)$ yields the integrated polynomial form

$$S_xJ(D_xD_y)(x,y)NM(C) = \frac{138(x)^{10}}{10} + \frac{84x^{13}}{13} + \frac{98(x)^{14}}{14} + \frac{120(x)^{16}}{16} + \frac{140(x)^{17}}{17},$$

(with the obvious simplifications for zero coefficients).

Combining the above expressions and evaluating at the specific numerical x, y-values used in our computations gives the numerical topological indices listed in Table 4. Hence the various TIs in Table 4 follow from these formulae.

Theorem 3.5 Let C be the graph of the molecule Carmustine (Cm). Then

$$M(C) = 3xy^2 + 2xy^3 + 2x^2y^2 + 3x^2y^3 + 2x^3y^3,$$

and

$$NM(C) = 2x^2y^3 + x^2y^4 + 2x^3y^5 + x^3y^6 + x^3y^7 + x^4y^7 + x^5y^6 + x^5y^7 + x^6y^7 + x^7y^7.$$

Proof: The graph of Carmustine (Cm) is shown in Figure-1. It has $|V(C)| = 13$ vertices and $e(C) = 12$ edges. We classify edges according to the degrees of their end-vertices. Let

$$e_{ij} = |\{uv \in E(Cm) \mid d(u) = i,\ d(v) = j,\ i \leq j\}|,$$

be the number of edges with end-vertex degrees i and j. For Carmustine, these classes are

$$e_{12} = 3, \quad e_{13} = 2, \quad e_{22} = 2, \quad e_{23} = 3, \quad e_{33} = 2.$$

By definition, M-polynomial is

$$M(C) = \sum_{a \leq b} m_{ab}(C)\, x^a y^b,$$

so substituting the nonzero e_{ij}values yields,

$$\begin{aligned} M(C) &= e_{12}x^1y^2 + e_{13}x^1y^3 + e_{22}x^2y^2 + e_{23}x^2y^3 + e_{33}x^3y^3 \\ &= 3xy^2 + 2xy^3 + 2x^2y^2 + 3x^2y^3 + 2x^3y^3, \end{aligned}$$

which proves the first formula.

For the neighborhood-degree polynomial, we classify edges by the sum (or some neighborhood-degree) classes; let

$$e^*_{ij} = \#\{uv \in E(Cm) \mid \mathrm{nd}(u) = i,\ \mathrm{nd}(v) = j,\ i \leq j\}.$$

For Carmustine the non-Möbius edge classes are

$$e^*_{23} = 2,\ e^*_{24} = 1,\ e^*_{35} = 2,\ e^*_{36} = 1,\ e^*_{37} = 1,\ e^*_{47} = 1,$$

$$e^*_{56} = 1,\ e^*_{57} = 1,\ e^*_{67} = 1,\ e^*_{77} = 1.$$

By definition

$$NM(C) = \sum_{a \leq b} m^*_{ab}(C)\, x^a y^b,$$

substituting the above values gives

$$\begin{aligned} NM(C) &= e^*_{23}x^2y^3 + e^*_{24}x^2y^4 + e^*_{35}x^3y^5 + e^*_{36}x^3y^6 + e^*_{37}x^3y^7 \\ &\quad + e^*_{47}x^4y^7 + e^*_{56}x^5y^6 + e^*_{57}x^5y^7 + e^*_{67}x^6y^7 + e^*_{77}x^7y^7 \\ &= 2x^2y^3 + x^2y^4 + 2x^3y^5 + x^3y^6 + x^3y^7 + x^4y^7 + x^5y^6 + x^5y^7 + x^6y^7 + x^7y^7, \end{aligned}$$

which proves the second formula. Hence the theorem.

Theorem 3.6 Let C be the graph of molecule Carmustine (Cm) then

S.N O	M-P Index	Value	NM-P Index	Value
1	M_1(C)	12	NM_1(C)	112
2	M_2(C)	56	NM_2(C)	273
3	mM_2(C)	3.388	$NmNM_2$(C)	0.8366
4	$ReZG_3$(C)	272	ND_3(C)	3010
5	F(C)	126	NF(C)	600
6	SDD(C)	28.667	ND_5(C)	27.12
7	H(C)	5.4667	NH(C)	2.8825
8	I(C)	12.1	NI(C)	26.5034

Table 5: TIs of Carmustine(Cm)

Proof: By Theorem 3.5, we obtain the following operator evaluations on the polynomial $M(C)$ and $NM(C)$.

$$(D_x + D_y)M(C) = 9xy^2 + 8xy^3 + 8x^2y^2 + 15x^2y^3 + 12x^3y^3,$$

$$(D_xD_y)M(C) = 6xy^2 + 6xy^3 + 8x^2y^2 + 18x^2y^3 + 18x^3y^3,$$

$$(S_xS_y)M(C) = \frac{3xy^2}{2} + \frac{2xy^3}{3} + \frac{2(x)^2y^2}{4} + \frac{3x^2y^3}{6} + \frac{2x^3y^3}{9},$$

$$(D_xD_y)(D_x + D_y)M(C) = 18xy^2 + 24xy^3 + 32x^2y^2 + 90x^2y^3 + 108x^3y^3,$$

$$(D_x^2 + D_y^2)M(C) = 15xy^2 + 20xy^3 + 16x^2y^2 + 39x^2y^3 + 36x^3y^3,$$

$$(D_xS_y + D_yS_x)M(C) = \frac{15xy^2}{2} + \frac{20xy^3}{3} + 4x^2y^2 + \frac{13x^2y^3}{2} + 4x^3y^3.$$

Some intermediate (summation / integral) operations used in the computations are

$$2\big(S_xJ(x,y)M(C)\big) = 2(x)^3 + 2(x)^4 + \frac{4x^5}{5} + \frac{2x^6}{3},$$

and

$$S_xJ(D_xD_y)(x,y)M(C) = \frac{6(x)^4}{3} + \frac{3(x)^4}{2} + 2(x)^4 + \frac{18x^5}{5} + \frac{9x^6}{3}.$$

For the polynomial $NM(C;x,y)$ we obtain:

$$\begin{aligned}(D_x + D_y)NM(C) = {} & 10x^2y^3 + 6x^2y^4 + 16x^3y^5 + 9x^3y^6 + 10x^3y^7 \\ & + 11x^4y^7 + 11x^5y^6 + 12x^5y^7 + 13x^6y^7 + 14x^7y^7,\end{aligned}$$

$$\begin{aligned}(D_xD_y)NM(C) = {} & 12x^2y^3 + 8x^2y^4 + 30x^3y^5 + 18x^3y^6 + 21x^3y^7 \\ & + 28x^4y^7 + 30x^5y^6 + 35x^5y^7 + 42x^6y^7 + 49x^7y^7,\end{aligned}$$

$$\begin{aligned}(D_x^2 + D_y^2)NM(C) = {} & 26x^2y^3 + 20x^2y^4 + 68x^3y^5 + 45x^3y^6 + 58x^3y^7 \\ & + 65x^4y^7 + 61x^5y^6 + 74x^5y^7 + 85x^6y^7 + 98x^7y^7,\end{aligned}$$

$$\begin{aligned}(D_xD_y)(D_x + D_y)NM(C) = {} & 60x^2y^3 + 48x^2y^4 + 240x^3y^5 + 162x^3y^6 + 210x^3y^7 \\ & + 308x^4y^7 + 330x^5y^6 + 420x^5y^7 + 546x^6y^7 + 686x^7y^7.\end{aligned}$$

The (cleaned) symmetric-sum evaluations are

$$(S_xS_y)NM(C) = \frac{2x^2y^3}{6} + \frac{x^2y^4}{8} + \frac{2x^3y^5}{15} + \frac{x^3y^6}{18} + \frac{x^3y^7}{21} + \frac{x^4y^7}{28} + \frac{x^5y^6}{30} + \frac{x^5y^7}{35} + \frac{x^6y^7}{42} + \frac{x^7y^7}{49},$$

and

$$\begin{aligned}(D_xS_y + D_yS_x)NM(C) = {} & \frac{65x^4y^7}{28} + \frac{13x^2y^3}{3} + \frac{5x^2y^4}{2} + \frac{68x^3y^5}{15} + \frac{5x^3y^6}{2} \\ & + \frac{58x^3y^7}{21} + \frac{61x^5y^6}{30} + \frac{74x^5y^7}{35} + \frac{85x^6y^7}{42} + 2.\end{aligned}$$

Finally, the summation/integral identities used in the NM computations are

$$2\big(S_xJ(x,y)NM(C)\big) = \frac{4x^5}{5} + \frac{x^6}{3} + \frac{x^8}{2} + \frac{2x^9}{9} + \frac{x^{10}}{5} + \frac{4x^{11}}{11} + \frac{2x^{12}}{12} + \frac{2x^{13}}{13} + \frac{2x^{14}}{14},$$

and

$$S_xJ(D_xD_y)(x,y)NM(C) = \frac{12x^5}{5} + \frac{8x^6}{6} + \frac{30x^8}{8} + \frac{18x^9}{9} + \frac{21x^{10}}{10} + \frac{28x^{11}}{11} + \frac{30x^{11}}{11} + \frac{35x^{12}}{12} + \frac{42x^{13}}{13} + \frac{49x^{14}}{14}.$$

So that we obtain various TIs as in table 5 from the above equations.

Theorem 3.7 Let E be the molecular graph of Ellence (E). Then

$$M(E) = 2xy^2 + 2xy^3 + xy^4 + 2x^2y^2 + 12x^2y^3 + 2x^2y^4 + 15x^3y^3 + x^3y^4,$$

$$\begin{aligned} NM(E) = {} & x^2y^3 + x^2y^4 + 2x^3y^6 + 7x^3y^7 + 2x^4y^5 + x^4y^7 + x^4y^8 \\ & + 3x^5y^6 + 2x^5y^7 + x^5y^8 + 2x^6y^6 + 2x^6y^7 + x^7y^7 \\ & + 6x^7y^8 + 8x^7y^9 + 2x^8y^9 + x^9y^9. \end{aligned}$$

Proof: The molecular graph of Ellence (E) is shown in Figure-1. From the structure we have $|V(E)| = 39$ and $|E(E)| = 43$.

Classify edges by the degrees of their end-vertices. For $i \leq j$ define

$$e_{ij} = \{uv \in E(E) \mid d(u) = i,\ d(v) = j\},$$

the number of edges whose end-vertex degrees are i and j. From the molecular structure the nonzero classes are

$$e_{12} = 2,\ e_{13} = 2,\ e_{14} = 1,\ e_{22} = 2,\ e_{23} = 12,\ e_{24} = 2,\ e_{33} = 15,\ e_{34} = 1.$$

By definition, an M-polynomial is

$$M(E) = \sum_{a \leq b} m_{ab}(E)\, x^a y^b,$$

so substituting the above e_{ij} values yields

$$\begin{aligned} M(E) &= e_{12}x^1y^2 + e_{13}x^1y^3 + e_{14}x^1y^4 + e_{22}x^2y^2 + e_{23}x^2y^3 \\ &\quad + e_{24}x^2y^4 + e_{33}x^3y^3 + e_{34}x^3y^4 \\ &= 2xy^2 + 2xy^3 + xy^4 + 2x^2y^2 + 12x^2y^3 + 2x^2y^4 + 15x^3y^3 + x^3y^4, \end{aligned}$$

which proves the first formula.

Next classify edges by the neighborhood-degree classes. For $i \leq j$ define

$$e^*_{ij} = \{uv \in E(E) \mid \mathrm{nd}(u) = i,\ \mathrm{nd}(v) = j\},$$

the number of edges whose endpoint neighborhood-degrees are i and j. The nonzero e^*_{ij} values are

$$\begin{gathered} e^*_{23} = 1,\ e^*_{24} = 1,\ e^*_{36} = 2,\ e^*_{37} = 7,\ e^*_{45} = 2,\ e^*_{47} = 1,\ e^*_{48} = 1, \\ e^*_{56} = 3,\ e^*_{57} = 2,\ e^*_{58} = 1,\ e^*_{66} = 2,\ e^*_{67} = 2,\ e^*_{77} = 1, \\ e^*_{78} = 6,\ e^*_{79} = 8,\ e^*_{89} = 2,\ e^*_{99} = 1. \end{gathered}$$

By definition the NM-polynomial is

$$NM(E) = \sum_{a \leq b} m^*_{ab}(E)\, x^a y^b,$$

and substituting the above e^*_{ij} values gives

$$\begin{aligned} NM(E) &= e^*_{23}x^2y^3 + e^*_{24}x^2y^4 + e^*_{36}x^3y^6 + e^*_{37}x^3y^7 + e^*_{45}x^4y^5 \\ &\quad + e^*_{47}x^4y^7 + e^*_{48}x^4y^8 + e^*_{56}x^5y^6 + e^*_{57}x^5y^7 + e^*_{58}x^5y^8 \\ &\quad + e^*_{66}x^6y^6 + e^*_{67}x^6y^7 + e^*_{77}x^7y^7 + e^*_{78}x^7y^8 + e^*_{79}x^7y^9 \\ &\quad + e^*_{89}x^8y^9 + e^*_{99}x^9y^9 \\ &= x^2y^3 + x^2y^4 + 2x^3y^6 + 7x^3y^7 + 2x^4y^5 + x^4y^7 + x^4y^8 \\ &\quad + 3x^5y^6 + 2x^5y^7 + x^5y^8 + 2x^6y^6 + 2x^6y^7 + x^7y^7 \\ &\quad + 6x^7y^8 + 8x^7y^9 + 2x^8y^9 + x^9y^9, \end{aligned}$$

which proves the second formula. Hence the theorem.

Theorem 3.8 Let E denote the graph representing molecule Ellence (E), then,

S.NO	M-P Index	Value	NM-P Index	Value
1	$M_1(E)$	220	$NM_1(E)$	544
2	$M_2(E)$	27	$NM_2(E)$	1767
3	$mM_2(E)$	8.14	$NmNM_2(E)$	1.483
4	$ReZG_3(E)$	1510	$ND_3(E)$	24926
5	$F(E)$	614	$NF(E)$	3758
6	$SDD(E)$	100.83	$ND_5(E)$	104.945
7	$H(E)$	17.4857	$NH(E)$	7.68
8	$I(E)$	51.4142	$NI(E)$	130.8141

Table 6: TIs of Ellence (E)

Proof: By using Theorem 3.7, we obtain the following equations:

$$(D_x + D_y)M(E) = 6xy^2 + 32xy^3 + 5xy^4 + 8x^2y^2 + 60x^2y^3 + 12x^2y^4 + 90x^3y^3 + 7x^3y^4,$$

$$(D_xD_y)M(E) = 4xy^2 + 24xy^3 + 4xy^4 + 8x^2y^2 + 72x^2y^3 + 16x^2y^4 + 135x^3y^3 + 12x^3y^4,$$

$$S_xS_yM(E) = xy^2 + \tfrac{8}{3}xy^3 + \tfrac{1}{4}xy^4 + \tfrac{1}{2}x^2y^2 + 2x^2y^3 + \tfrac{1}{4}x^2y^4 + \tfrac{15}{9}x^3y^3 + \tfrac{1}{12}x^3y^4,$$

$$(D_xD_y)(D_x + D_y)M(E) = 12xy^2 + 96xy^3 + 20xy^4 + 32x^2y^2 + 360x^2y^3 + 96x^2y^4 + 810x^3y^3 + 84x^3y^4,$$

$$(D_x^2 + D_y^2)M(E) = 10xy^2 + 80xy^3 + 17xy^4 + 16x^2y^2 + 156x^2y^3 + 40x^2y^4 + 270x^3y^3 + 25x^3y^4,$$

$$(D_xS_y + D_yS_x)M(E) = 5xy^2 + \tfrac{80}{3}xy^3 + \tfrac{17}{4}xy^4 + 4x^2y^2 + 26x^2y^3 + 5x^2y^4 + 30x^3y^3 + \tfrac{25}{12}x^3y^4.$$

$$2\left[S_xJ(x,y)M(E)\right] = \tfrac{4}{3}x^3 + 4x^4 + \tfrac{2}{5}x^5 + x^4 + \tfrac{24}{5}x^5 + \tfrac{2}{3}x^6 + 5x^6 + \tfrac{2}{7}x^7.$$

$$S_xJD_xD_y(x,y)N(E) = \tfrac{4}{3}x^3 + 8x^4 + \tfrac{76}{5}x^5 + \tfrac{151}{6}x^6 + \tfrac{12}{7}x^7.$$

$$\begin{aligned}(D_x + D_y)NM(E) = {} & 5x^2y^3 + 6x^2y^4 + 18x^3y^6 + 70x^3y^7 + 18x^4y^5 + 11x^4y^7 + 12x^4y^8 \\ & + 33x^5y^6 + 24x^5y^7 + 13x^5y^8 + 24x^6y^6 + 26x^6y^7 + 14x^7y^7 \\ & + 90x^7y^8 + 128x^7y^9 + 34x^8y^9 + 18x^9y^9,\end{aligned}$$

$$\begin{aligned}(D_xD_y)NM(E) = {} & 6x^2y^3 + 8x^2y^4 + 36x^3y^6 + 147x^3y^7 + 40x^4y^5 + 28x^4y^7 + 32x^4y^8 \\ & + 90x^5y^6 + 70x^5y^7 + 40x^5y^8 + 72x^6y^6 + 84x^6y^7 + 49x^7y^7 \\ & + 336x^7y^8 + 504x^7y^9 + 144x^8y^9 + 81x^9y^9.\end{aligned}$$

$$\begin{aligned}(D_x^2 + D_y^2)NM(E) = {} & 13x^2y^3 + 20x^2y^4 + 90x^3y^6 + 406x^3y^7 + 82x^4y^5 + 65x^4y^7 + 80x^4y^8 \\ & + 183x^5y^6 + 148x^5y^7 + 89x^5y^8 + 144x^6y^6 + 170x^6y^7 + 98x^7y^7 \\ & + 678x^7y^8 + 1040x^7y^9 + 290x^8y^9 + 162x^9y^9.\end{aligned}$$

$$(D_xD_y)(D_x+D_y)NM(E) = 30x^2y^3+48x^2y^4+32x^3y^6+1470x^3y^7+360x^4y^5+308x^4y^7+384x^4y^8 + 990x^5y^6+840x^5y^7+520x^5y^8+864x^6y^6+1092x^6y^7+686x^7y^7 + 5040x^7y^8+8064x^7y^9+2448x^8y^9+1458x^9y^9.$$

$$(S_xS_y)NM(E) = \tfrac{1}{6}x^2y^3+\tfrac{1}{8}x^2y^4+\tfrac{1}{9}x^3y^6+\tfrac{1}{3}x^3y^7+\tfrac{1}{10}x^4y^5+\tfrac{1}{28}x^4y^7+\tfrac{1}{32}x^4y^8+\tfrac{1}{10}x^5y^6+\tfrac{2}{35}x^5y^7 + \tfrac{1}{40}x^5y^8+\tfrac{1}{18}x^6y^6+\tfrac{1}{49}x^7y^7+\tfrac{3}{28}x^7y^8+\tfrac{8}{63}x^7y^9+\tfrac{1}{36}x^8y^9+\tfrac{1}{81}x^9y^9.$$

$$(D_xS_y+D_yS_x)NM(E) = \tfrac{13}{6}x^2y^3+\tfrac{5}{2}x^2y^4+5x^3y^6+\tfrac{58}{3}x^3y^7+\tfrac{41}{10}x^4y^5+\tfrac{65}{28}x^4y^7+\tfrac{5}{2}x^4y^8 + \tfrac{61}{10}x^5y^6+\tfrac{148}{35}x^5y^7+\tfrac{89}{40}x^5y^8+4x^6y^6+\tfrac{85}{21}x^6y^7+2x^7y^7 + \tfrac{339}{28}x^7y^8+\tfrac{1040}{63}x^7y^9+\tfrac{145}{36}x^8y^9+2x^9y^9.$$

$2[S_xJ(x,y)NM(E)] = \frac{2}{5}x^5+\frac{1}{3}x^6+\frac{8}{9}x^9+\frac{14}{10}x^{10}+\frac{8}{11}x^{11}+\frac{10}{12}x^{12}+\frac{6}{13}x^{13}+\frac{2}{14}x^{14}+\frac{12}{15}x^{15}+x^{16}+\frac{4}{17}x^{17}+\frac{2}{18}x^{18}.$
$S_xJD_xD_y(x,y)NM(E) = \frac{6}{5}x^5+\frac{8}{6}x^6+\frac{76}{9}x^9+\frac{147}{10}x^{10}+\frac{118}{11}x^{11}+\frac{174}{12}x^{12}+\frac{124}{13}x^{13}+\frac{49}{14}x^{14}+\frac{336}{15}x^{15}+\frac{504}{16}x^{16}+\frac{144}{17}x^{17}+\frac{81}{18}x^{18}.$

So that we obtain various TIs as in Table 5 from the above equations.

Theorem 3.9 Let H be the graph of molecule Hydroxyurea (H), then

$$M(H) = xy^2+2xy^3+x^2y^3, \quad NM(H) = x^2y^4+2x^3y^4+x^4y^4.$$

Proof: The molecular graph of Hydroxyurea (H), represented in Figure 1. We have number of vertices $V(H)=5$ and number of edges $e(H)=4$. The edge set of Hydroxyurea (H) is divided into 3 classes on the basis of degree of vertices as follows:

$$e_{12}=1, \quad e_{13}=2, \quad e_{23}=1.$$

$$M(H) = \sum_{a\leq b} m_{ab}(A)x^ay^b = e_{12}x^1y^2+e_{13}x^1y^3+e_{23}x^2y^3 = xy^2+2xy^3+x^2y^3.$$

Similarly, considering the sum of the degrees of neighborhood vertices, the edge set of Hydroxyurea (H) is divided into 3 classes as follows:

$$e^*_{24}=1, \quad e^*_{36}=2, \quad e^*_{34}=2, \quad e^*_{44}=1.$$

$$NM(H) = \sum_{a\leq b} m^*_{ab}(A)x^ay^b = e^*_{24}x^2y^4+e^*_{34}x^3y^4+e^*_{44}x^4y^4$$

NM(H)= $x^2y^4+2x^3y^4+x^4y^4$. Hence the theorem.

Theorem 3.10 Let H denote the graph representing molecule Hydroxyurea (H). then

M-P Indices			**NM-P Indices**	
S.NO	**Index**	**Value**	**Index**	**Value**
1	$M_1(H)$	16	$NM_1(H)$	28
2	$M_2(H)$	14	$NM_2(H)$	48
3	$mM_2(H)$	1.33	$NnmM_2(H)$	0.3541
4	$ReZG_3(H)$	60	$ND_3(H)$	344
5	$F(H)$	38	$NF(H)$	102
6	$SDD(H)$	11.33	$ND_s(H)$	8.66
7	$H(H)$	2.0667	$NH(H)$	1.1547
8	$I(H)$	3.3666	$NI(H)$	6.7619

Table 7: Topological indices (TIs) of Hydroxyurea (H).

Proof: By using Theorem 3.9 we obtain the following operator relations for $M(H;x,y)$ and $NM(H)$:

$$\big(D_x+D_y\big)M(H)=3xy^2+8xy^3+5x^2y^3,$$

$$\big(D_xD_y\big)M(H)=2xy^2+6xy^3+6x^2y^3,$$

$$S_xS_yM(H)=\frac{xy^2}{2}+\frac{2xy^3}{3}+\frac{x^2y^3}{6},$$

$$\big(D_xD_y\big)\big(D_x+D_y\big)M(H)=6xy^2+24xy^3+30x^2y^3,$$

$$\big(D_x^2+D_y^2\big)M(H)=5xy^2+20xy^3+13x^2y^3,$$

$$\big(D_xS_y+D_yS_x\big)M(H)=\frac{5xy^2}{2}+\frac{20xy^3}{3}+\frac{13x^2y^3}{6},$$

$$2\big[S_xJ(x,y)M(H)\big]=\frac{2x^3}{3}+x^4+\frac{2x^5}{5},$$

$$S_xJD_xD_y(x,y)N(H)=\frac{2(x)^3}{3}+\frac{6(x)^4}{4}+\frac{6(x)^5}{5}.$$

Similarly, for the NM-polynomial $NM(H;x,y)$ we get

$$\big(D_x+D_y\big)NM(H)=6x^2y^4+14x^3y^4+8x^4y^4,$$

$$\big(D_xD_y\big)NM(H)=8x^2y^4+24x^3y^4+16x^4y^4,$$

$$\big(D_x^2+D_y^2\big)NM(H)=20x^2y^4+50x^3y^4+32x^4y^4,$$

$$\big(D_xD_y\big)\big(D_x+D_y\big)NM(H)=48x^2y^4+168x^3y^4+128x^4y^4,$$

$$S_xS_yNM(H)=\frac{x^2y^4}{8}+\frac{x^3y^4}{6}+\frac{x^4y^4}{16},$$

$$\big(D_xS_y+D_yS_x\big)NM(H)=\frac{5x^2y^4}{2}+\frac{25x^3y^4}{6}+2x^4y^4,$$

$$2\big[S_xJ(x,y)NM(H)\big]=\frac{x^6}{3}+\frac{4(x)^7}{7}+\frac{x^8}{4},$$

$$S_xJD_xD_y(x,y)NM(H)=\frac{4x^6}{3}+\frac{24x^7}{7}+2x^8.$$

4. Result and Discussion

Quantitative structure analysis of chemical graphs of Adriamycin (A), Ellence (E), Carboplatin (Cb), Hydroxyurea (H), and Carmustine (Cm) Using certain physicochemical characteristics of the medications Adriamycin (A), Ellence (E), Carboplatin (Cb), Hydroxyurea (H), and Carmustine (Cm), as well as the TIs they yield, QSPR modelling has been performed in this section. The model considers 10 physicochemical parameters, namely: molar weight, melting point, pKa values, half-life, logP, heat of formation, boiling point, density, polar surface area, and refractive index, together with 16 TIs (eight degree-based (DB) and eight neighborhood degree sum-based (NDSB)) as listed in Table 2. MATLAB software was employed to obtain the curvilinear regression analysis. The values of the TIs of the cancer treatment medications are taken as the independent variables in the regression models.

Drug	**M1**	**M2**	**mM2**	**F**	**$ReZA_3/ND_3$**	**$SDdeg/ND_5$**	**I**	**H**
Adriamycin	228	286	8.55	652	1596	108	52.6952	17.7044
Carboplatin	74	90	2.67	1260	8144	37.67	16.2619	5.5047
Carmustine	52	56	3.388	126	272	28.667	12.1	5.4667
Ellence	220	275	8.146	614	1510	103	51.4142	17.4857
Hydroxyurea	16	14	4.88	38	60	11	3.366	2.0666

Table 8: Various Anti-cancer drugs with DB TIs values

Drug	**NM1**	**NM2**	**NmM2**	**NF**	**ND_3**	**ND_5**	**NI**	**NH**	**NM1**
Adriamycin	572	1908	1.4160	4054	27618	97.45	137.5879	7.2698	572
Carboplatin	180	580	0.412	1260	8144	31.03	42.9968	2.2787	180
Carmustine	112	273	0.8367	600	3010	27.12	6.7619	2.8825	112
Ellence	544	1767	1.483	3758	24926	95.1654	130.8141	7.36	544
Hydroxyurea	28	48	0.3541	102	344	8.666	6.7619	1.1547	28

Table 9: Various anti-cancer drugs with NDSB TIs values.

The following regression models are examined in this study:

$$Y = A + Bx_1 \qquad \text{(Linear polynomial)},$$
$$Y = A + Bx_2 + Cx_2^2 \qquad \text{(Quadratic polynomial)},$$
$$Y = A + Bx_3 + Cx_3^2 + Dx_3^3 \qquad \text{(Cubic polynomial)},$$

where Y is the response variable, A is the regression constant, and B, C, D are the coefficients for the individual descriptors. Here x_1, x_2, x_3 represent independent variables, n is the number of samples used to construct the regression equation, R is the correlation coefficient, SE is the standard error, and F denotes Fisher's statistic.

It is well known that when theoretical and experimental outcomes are extremely similar, the correlation coefficient R approaches 1. To assess the model's predictive quality, the observed values and model predictions must be compared. For predictive performance, the RMSE (Root Mean Square Error) statistic is used. The model with the smallest RMSE value is considered the best prediction model. The RMSE is defined as:

$$\text{RMSE} = \sqrt{\frac{1}{n}\sum_{i=1}^{n}(z_i - \bar{z}_i)^2},$$

where z_i represents the observed value of the independent variable in the test set, $\bar{z}_i$ denotes the corresponding predicted value, and n is the number of test samples.

Based on linear, quadratic, and cubic regression models, Tables 10, 11, and 12 present the correlation coefficient (R) values between TIs and the physicochemical properties of the cancer therapy medicines. In these tables, the bold entries indicate the highest R value for each physicochemical parameter.

TI/Prop	MW	MP	*pKa*	HL	*LogP*	HF	BP	D	PSA	RI
M1	0.9528	0.7020	0.6660	0.6059	0.6790	0.8029	0.9555	-0.6247	0.9677	0.7188
M2	**0.9546**	**0.7144**	**0.6756**	0.6074	0.6684	0.8073	**0.9601**	-0.6518	**0.9716**	0.7247
mM2	-0.6444	-0.1610	0.2362	-0.1239	-0.7926	-0.7420	-0.4042	**0.9124**	-0.3412	0.7338
F	0.5940	0.7093	0.2826	0.1124	0.0938	**0.8181**	0.5448	-0.2813	0.4561	**0.8892**
$ReZA_3$	0.2457	0.4660	0.0251	-0.1338	-0.1705	0.5458	0.1907	-0.0514	0.0926	0.6555
$SD_{\deg}$	0.9538	0.6960	0.6572	**0.6133**	0.6870	0.8032	0.9526	-0.6330	0.9647	0.7187
l	0.9487	0.6930	0.6615	0.6000	0.6848	0.7951	0.9512	-0.6275	**0.9648**	0.7093
H	0.9338	0.6488	0.6355	0.5939	**0.7133**	0.7668	0.9307	-0.6463	0.9486	0.6748

Table 10: The linear regression model's correlation coefficient (R) values between TIs and the physicochemical characteristics of several cancer treatment medications.

TI/Prop	MW	MP	Pka	HL	LogP	HF	BP	D	PSA	RI
M1	0.9540	0.8740	0.2990	**0.888**	0.5450	0.8590	0.9930	-0.5301	0.9652	0.8472
M2	0.9492	**0.8812**	0.3132	0.8951	0.5323	0.8522	**0.9953**	-0.5174	**0.9681**	0.8386
mM2	-0.7481	-0.0332	**0.6642**	-0.0632	-0.9991	-0.8801	-0.4133	**0.9992**	-0.2722	-0.8921
F	0.9591	0.4541	-0.2842	0.4811	0.9202	**0.9981**	0.7611	-0.9132	0.6552	**0.9991**
ReZA3	0.8761	0.2532	-0.4823	0.2833	**0.9821**	0.9642	0.6051	-0.9792	0.4781	0.9692
SDdeg	0.9561	0.8692	0.2891	0.8841	0.5532	0.8651	0.9921	-0.5391	0.9622	0.8523
I	0.9551	0.8721	0.2952	0.8871	0.5482	0.8622	0.9932	-0.5332	0.9643	0.8482
H	**0.9611**	0.8612	0.2743	0.8762	0.5672	0.8723	0.9901	-0.5523	0.9583	0.8604

Table 11: The quadratic regression model's correlation coefficient (R) values between TIs and the physicochemical characteristics of several cancer treatment medications.

TI/Prop	MW	MP	Pka	HL	LogP2	HF	BP	D	PSA	RI
M1	0.9501	0.7840	0.6013	0.7137	0.8223	0.7842	0.9897	-0.7141	0.9885	0.6792
M2	0.9502	**0.7906**	**0.6067**	**0.7211**	0.8177	0.7841	**0.9911**	- 0.7096	**0.9899**	0.6795
mM2	-0.6799	-0.1378	0.4088	-0.1399	-0.8315	-0.8665	-0.4316	**0.9313**	-0.3435	-0.8966
F	0.4078	0.2334	-0.4027	0.3155	0.3501	0.6818	0.1765	-0.5206	0.0701	**0.7891**
ReZ_{A_J}	-0.0834	-0.1728	-0.6755	-0.0662	-0.0683	0.2529	-.3198	-0.1430	-0.4183	0.4034
SDdeg	**0.9532**	0.7859	0.5966	0.7166	0.8247	**0.7905**	0.9905	-0.7185	0.9881	0.6868
I	0.9465	0.7756	0.6066	0.7035	0.8240	0.7778	0.9873	-0.7138	0.9873	0.6711
H	0.9385	0.7535	0.5942	0.6775	**0.8300**	0.7650	0.9805	-0.7160	0.9828	0.6549

Table 12: The cubic regression model's correlation coefficient (R) values between TIs and the physicochemical characteristics of several cancer treatment medications

From Table 10, M_2 for Molar weight, M_2 for Melting point, M_2 for pK_a, $SD_{\deg}$ for Half-life, H for LogP, F index for Heat of Formation, M_2 index for Boiling point, mM_2 index for Density, M_2 for PSA and F in Refractive Index are the best estimator indices in linear regression models. The linear models obtained with these TIs are as follows:

$$\text{MW} = 1.6166M_2 + 123.1473 \quad F\text{-ratio: } 30.8010 \quad \text{SE: } 74.1962 \quad \text{RMSE: } 57.4722 \tag{4.1}$$

$$\text{MP} = 0.3699M_2 + 111.0622 \quad F\text{-ratio: } 3.1275 \quad \text{SE: } 53.2771 \quad \text{RMSE: } 41.2683 \tag{4.2}$$

$$\text{p}K_a = 0.0110M_2 + 6.2597 \quad F\text{-ratio: } 2.5192 \quad \text{SE: } 1.7588 \quad \text{RMSE: } 1.3623 \tag{4.3}$$

$$\text{HL} = 0.1963SD_{\deg} - 2.9225 \quad F\text{-ratio: } 1.8090 \quad \text{SE: } 13.0626 \quad \text{RMSE: } 10.1183 \tag{4.4}$$

$$\text{LogP} = 0.1165H - 0.6174 \quad F\text{-ratio: } 3.1068 \quad \text{SE: } 0.9766 \quad \text{RMSE: } 0.7565 \tag{4.5}$$

$$\text{HF} = 0.0653F - 51.3419 \quad F\text{-ratio: } 6.0703 \quad \text{SE: } 25.9734 \quad \text{RMSE: } 20.1189 \tag{4.6}$$

$$\text{BP} = 1.0116M_2 + 242.4426 \quad F\text{-ratio: } 35.3204 \quad \text{SE: } 43.3592 \quad \text{RMSE: } 33.5859 \tag{4.7}$$

$$\text{D} = 0.0055mM_2 + 1.2056 \quad F\text{-ratio: } 14.9051 \quad \text{SE: } 0.0549 \quad \text{RMSE: } 0.0425 \tag{4.8}$$

$$\text{PSA} = 0.5599M_2 + 49.1316 \quad F\text{-ratio: } 50.6295 \quad \text{SE: } 20.0435 \quad \text{RMSE: } 15.5256 \tag{4.9}$$

$$\text{RI} = 0.0001F + 1.5853 \quad F\text{-ratio: } 11.3304 \quad \text{SE: } 0.0329 \quad \text{RMSE: } 0.0255 \tag{4.10}$$

From Table 11, M_2 for Molar weight, Melting point, Half-life, Boiling point and PSA, mM_2 for pK_a and Density, ReZ for LogP, F index for Heat of Formation, and F in Refractive Index are the best estimator indices in Quadratic regression models. The Quadratic models obtained with these TIs are as follows:

$$\text{MW} = -2.6962H^2 + 84.5235H - 90.3671 \quad F\text{-ratio: } 13.5586 \quad \text{SE: } 79.9415 \quad \text{RMSE: } 50.5594 \tag{4.11}$$

$$\text{MP} = -0.0010M_2^2 + 0.6828M_2 + 98.9846 \quad F\text{-ratio: } 1.0770 \quad \text{SE: } 64.7071 \quad \text{RMSE: } 40.9244 \tag{4.12}$$

$$\text{p}K_a = -0.0143mM_2^2 + 0.7802mM_2 + 3.8518 \quad F\text{-ratio: } 1.9097 \quad \text{SE: } 1.7128 \quad \text{RMSE: } 1.0833 \tag{4.13}$$

$$\text{HL} = 0.0007M_2^2 - 0.1421M_2 + 6.6697 \quad F\text{-ratio: } 0.8078 \quad \text{SE: } 15.0651 \quad \text{RMSE: } 9.5280 \tag{4.14}$$

$$\text{LogP} = -0.0000\text{ReZ}^2 + 0.0013\text{ReZ} - 0.2861 \quad F\text{-ratio: } 0.9145 \quad \text{SE: } 1.2334 \quad \text{RMSE: } 0.7801 \tag{4.15}$$

$$\text{HF} = -0.0001F^2 + 0.2128F - 74.6490 \quad F\text{-ratio: } 82.1943 \quad \text{SE: } 6.0642 \quad \text{RMSE: } 3.8354 \tag{4.16}$$

$$\text{BP} = -0.0017M_2^2 + 1.5454M_2 + 221.8424 \quad F\text{-ratio: } 12.7779 \quad \text{SE: } 51.1317 \quad \text{RMSE: } 32.3386 \tag{4.17}$$

$$\text{D} = 0.0003mM_2^2 - 0.0104mM_2 + 1.2822 \quad F\text{-ratio: } 11.1015 \quad \text{SE: } 0.0472 \quad \text{RMSE: } 0.0299 \tag{4.18}$$

$$\text{PSA} = 0.0002M_2^2 + 0.4802M_2 + 52.2092 \quad F\text{-ratio: } 17.0137 \quad \text{SE: } 24.4546 \quad \text{RMSE: } 15.4664 \tag{4.19}$$

$$\text{RI} = -0.0000F^2 + 0.0003F + 1.5559 \quad F\text{-ratio: } 110.2240 \quad \text{SE: } 0.0083 \quad \text{RMSE: } 0.0053 \tag{4.20}$$

From min (RMSE) and max(R), the F index for the Refractive Index and mM_2 for Density is the best predictive topological index in the quadratic models. From min (RMSE) and max(R), Tables 10 and 11 show that quadratic models have predicted ability better than linear models.
From Table 12, SD_{deg} index for Molar weight and Half-life, M_2 index for MP, pK_a, Half-life, Boiling point and PSA, H for LogP, mM_2 for Density and F for Refractive index are the best predictive TIs in the cubic regression models. The cubic regression models of these indices are as follows:

$$\text{MW} = 0.0003SD_{\text{deg}}^3 - 0.122SD_{\text{deg}}^2 + 15.464SD_{\text{deg}} - 93.075$$
$$F\text{-ratio: } 15.307 \quad \text{SE: } 62.973 \quad \text{RMSE: } 28.1624 \tag{4.21}$$

$$\text{MP} = -0.0001M_2^3 + 0.0393M_2^2 - 2.5414M_2 + 148.3188$$
$$F\text{-ratio: } 0.6543 \quad \text{SE: } 76.6163 \quad \text{RMSE: } 34.2638 \tag{4.22}$$

$$\text{p}K_a = -0.0000M_2^3 + 0.0015M_2^2 - 0.138M_2 + 9.5621$$
$$F\text{-ratio: } 1.15 \quad \text{SE: } 1.9587 \quad \text{RMSE: } 0.8759 \tag{4.23}$$

$$\text{HL} = 0.0000M_2^3 - 0.0137M_2^2 + 1.0084M_2 - 10.9335$$
$$F\text{-ratio: } 1.6911 \quad \text{SE: } 11.6239 \quad \text{RMSE: } 5.1984 \tag{4.24}$$

$$\text{LogP} = 0.0033H^3 - 0.1153H^2 + 1.2878H - 3.5125$$
$$F\text{-ratio: } 1.2556 \quad \text{SE: } 1.1054 \quad \text{RMSE: } 0.4944 \tag{4.25}$$

$$\text{HF} = -0.0002SD_{\text{deg}}^3 + 0.0007SD_{\text{deg}}^2 + 2.9447SD_{\text{deg}} - 107.8180$$
$$F\text{-ratio: } 3.3211 \quad \text{SE: } 23.6247 \quad \text{RMSE: } 10.5653 \tag{4.26}$$

$$\text{BP} = -0.0001M_2^3 + 0.0328M_2^2 - 1.2125M_2 + 264.0410$$
$$F\text{-ratio: } 6.7362 \quad \text{SE: } 58.2829 \quad \text{RMSE: } 26.0649 \tag{4.27}$$

$$\text{D} = -0.0004mM_2^3 + 0.0268mM_2^2 - 0.2639mM_2 + 1.8143$$
$$F\text{-ratio: } 21.2964 \quad \text{SE: } 0.0288 \quad \text{RMSE: } 0.0129 \tag{4.28}$$

$$\text{PSA} = -0.0000M_2^3 + 0.0184M_2^2 - 0.9702M_2 + 74.4015$$
$$F\text{-ratio: } 10.0846 \quad \text{SE: } 26.2558 \quad \text{RMSE: } 11.7419 \tag{4.29}$$

$$\text{RI} = 0.0000F^3 - 0.0000F^2 + 0.0006F + 1.5394$$
$$F\text{-ratio: } 60727.5686 \quad \text{SE: } 0.0003 \quad \text{RMSE: } 0.0001 \tag{4.30}$$

From min (RMSE) and max(R), the mM_2 index for Density and F index for Refractive index are the best predictive TIs in the cubic models. From min (RMSE) and max(R), Table 11 and Table 12 show that cubic models have predicted ability better than quadratic models. Here the bold values represented in Table 10, 11, 12 show the highest values of correlation between TI's and properties.

5. Conclusion

The properties of the molecular structure, which can be ascertained via QSPR modelling with TIs, are critical to the success of a novel product in pharmaceutical drug design. Using the edge partition technique and analysing their molecular makeup, the expressions of M-P and NM-P are established for several interesting multi-target medications, including Adriamycin (A), Carboplatin (Cb), Carmustine (Cm), Ellence(E) and Hydroxyurea (H), These polynomials are also used to create several DB and NDSB TIs since there is a strong correlation between these TIs mentioned in table 1 and the molecular structures of some medications used to treat cancer. QSPR models for Molar weight, melting point, pka values, half-life, logP, heat of formation, boiling point, density, polar surface area, and refractive index. The values of the chosen TIs are used to determine the attributes of the multi-target medications Adriamycin(A), Carboplatin (Cb), Carmustine (Cm), Ellence (E) and Hydroxyurea(H), which in the treatment of cancer, including curvilinear regression models are used to determine the association between TIs and these attributes. QSPR modelling shows that the best predictive TIs as: 1. Second Zagreb index in linear regression, quadratic regression, and cubic regression models for Melting point, Polar surface area. Boiling point. and Density. linear regression and cubic regression models for Pka value, in quadratic regression and cubic regression models for Half-life. and finally only linear regression for molar weight. 2. Forgotten topological index in linear regression, quadratic regression, and cubic regression models for refractive Index. in linear regression and quadratic regression models for Heat of formation 3. Harmonic index in quadratic regression models for molar weight., in linear regression and cubic regression models for LogP 4. Symmetric division index in linear regression models for Half -life and cubic regression models for molar weight, and Heat of formation. 5. Redefined third Zagreb index in quadratic regression models for LogP. In recent years, these medications have gained importance in the treatment of cancer. The findings of this study will provide insight into novel medication discoveries, particularly in the fields of chemistry, pharmaceutical science, and cancer treatment.

The limitions of study: There are still some constraints that need to be understood, even if the outcomes of this study are promising. The dataset is tiny, with only five anticancer drugs, which is the biggest problem. This makes the models less statistically powerful and less useful in other circumstances. Also, the regression models used here only use one topological descriptor at a time, so they don't completely show how a molecule's properties are often altered by a mix of structural, electronic, and physicochemical factors. We only looked at degree-based and neighbourhood-degree-sum-based topological indices. Spatial (3D) and quantum chemical descriptors were not included. It is tougher to tell how reliable a prediction is because there are no external validation methods like cross-validation or test set prediction. Changes or uncertainties in property data obtained from literature sources may introduce noise into experiments, thereby impacting the reliability of a model. So, the results should be seen as preliminary and suggestive, not certain.

Future Research: Future research can build on what has previously been done to overcome the flaws listed above and make QSPR modelling even better at predicting things. It would be a lot easier to validate the statistics if more anticancer drug molecules were added to the dataset. Adding new topological, geometrical, and quantum mechanical descriptors can improve the representation of structural variation and help us understand how structure and property are related. Multivariate regression analysis and advanced machine learning techniques like Support Vector Regression, Random Forest, Partial Least Squares Regression, or Neural Networks could help us find more accurate predictions of difficult, nonlinear relationships. Also, strict validation methods like k-fold cross-validation, external test set assessment, and Y-randomization must be used to make sure that the models can be used in other situations. You can adapt the idea to QSAR modelling by directly linking descriptors to biological activities, like IC50 values or molecular docking scores. This helps with rational drug design and optimization in cancer treatment.

Data availability statement: The raw data supporting the conclusions of this article will be made available by the authors, without undue reservation

Funding: The author(s) declare that no financial support was received for the research, authorship, and/or publication of this article.

Conflict of interest: The authors declare that the research was conducted in the absence of any commercial or financial relationships that could be construed as a potential conflict of interest.

References

1. Wiener, H. (1947). Correlation of heats of isomerization and differences in heats of combustion of isomeric hydrocarbons. *Journal of the American Chemical Society*, 69, 17.

2. Gutman, I., Ruscic, B., Trinajstić, N., & Wilcox, C. F. Jr. (1975). Graph theory and molecular orbitals. *Journal of Chemical Physics*, 62(9), 3399.
3. Manzoor, S., Siddiqui, M. K., & Ahmad, S. (2020). On entropy measures of molecular graphs using topological indices. *Arabian Journal of Chemistry*, Volume 13, Issue 8, 6285–6298.
4. Poojary, P., Raghavendra, A., Shenoy, B. G., Farahani, M. R., & Sooryanarayana, B. (2021). Certain topological indices and polynomials for the Isaac graphs. *Journal of Discrete Mathematical Sciences & Cryptography*, 24(2), 511–525.
5. Ahmad S., Siddiqui, H. M. A., Ali, A., Farahani, M. R., Imran, M., & Cangul, I. N. (2019). On Wiener index and Wiener polarity index of some polyomino chains. *Journal of Discrete Mathematical Sciences and Cryptography*, 22(7), 1151–1164.
6. Chen L., Mehboob, A., Ahmad, H., Nazeer, W., Hussain, M., & Farahani, M. R. (2019). Hosoya and Harary Polynomials of TOX(n), RTOX(n), TSL(n) and RTSL(n). *Discrete Dynamics in Nature & Society*, 2019, 1–18.
7. Ghorbani M., & Jalali, M. (2009). The Vertex PI, Szeged and Omega Polynomials of Carbon Nanocones CNC4[n]. *MATCH Communications in Mathematical and Computer Chemistry*, 62(2), 353–362.
8. Saleh A., Shalini, G. B. S., & Dhananjayamurthy, B. V. (2020). The reduced neighborhood topological indices and RNM-polynomial for the treatment of covid-19. *Open Chemistry*, 19(21): 2223–229.
9. Amin S., Rehman, M. A. U., Aldemir, M. S., Cancan, M., & Farahani, M. R. (2020). M-polynomial and degree based topological indices and line graph of hex board graph. *Eurasian Chemical Communications*, Vol. 2, Issue 12, 1156–1163.
10. Basavanagoud B., & Jakkannavar, P. (2020). M-Polynomial and degree based topological indices of graphs. *Electronic Journal of Mathematical Analysis & Applications*, 8(1), 75–99.
11. Afzal F., Hussain, S., Afzal, D., & Razaq, S. (2020). Some new degree based topological indices via M-polynomial. *Journal of Information and Optimization Sciences*, 41(4), 1061–1076.
12. Zuo X., Numan, M., Butt, S. I., Siddiqui, M. K., Ullah, R., & Ali, U. (2020). Computing Topological Indices for Molecules Structure of Polyphenylene via M-Polynomials. *Polycyclic Aromatic Compounds*, 42(4), 1103–1112.
13. Deutsch E., & Klavžar, S. (2015). M-polynomial and Degree-based Topological Indices. *Iranian Journal of Mathematical Chemistry*, 6(2), 93–102.
14. Shanmukha M. C., Basavarajappa, N. S., & Shilpa, K. C. (2020). Degree-based topological indices on anticancer drugs with QSPR analysis. *Heliyon*, 6, e04235.
15. Kirmani S. A. K., Ali, P., & Azam, F. (2021). Topological indices and QSPR/QSAR analysis of some antiviral drugs being investigated for the treatment of COVID-19 patients. *International Journal of Quantum Chemistry*, 121(9).
16. Bokhary S. A. U. H., Adnan, M. K., Siddiqui, M., & Cancan, M. (2021). On Topological Indices and QSPR Analysis of Drugs Used for the Treatment of Breast Cancer. *Polycyclic Aromatic Compounds*, 1–21.
17. Havare Ö. Ç. (2021). Topological indices and QSPR modeling of some novel drugs used in the cancer treatment. *International Journal of Quantum Chemistry*, 121(24), 1–23.
18. Hosamani S. M., Perigidad, D., Maled, S. J. Y., & Gavade, S. (2017). QSPR Analysis of Certain Degree Based Topological Indices. *Journal of Statistics Applications & Probability*, 6(2), 361–371.
19. https://www.chemspider.com/Chemical-Structure

Naveen S. Sapare.,
Department of of Engineering Mathematics,
Faculty of Engineering Mathematics, KLE Technological University Hubballi-580031, Karnataka, India.
E-mail address: naveen.sapare@kletech.ac.in

and

Sudhir R. Jog.,
Dept of Engineering Mathematics,
Faculty of Engineering Mathematics, Gogte Institute of Technology, Belagavi, Karnataka, India.
E-mail address: sudhir@git.edu

and

V. G. Hiremath.,
Department of Mathematics,
Faculty of Engineering Mathematics, KLE Technological University Hubballi-580031, Karnataka, India.
E-mail address: hveerabhadrayya@gmail.com

and

Vishwanath A. Modagi.,
Department of Mathematics,

Faculty of Engineering Mathematics, Jain College of engineering, Karnataka, India.
E-mail address: vmodagi99@gmail.com

and

Affiliated to,
Visvesvaraya Technological University,Belagavi-590018 Karnataka, India.